.

SUPPLEMENTAL MATERIALS

Shortening of titin's elastic tandem Ig segment leads to diastolic dysfunction

Short Title: Stiffer titin leads to diastolic dysfunction

Charles S Chung, PhD*[1]; Kirk R Hutchinson, PhD*[1]; Mei Methawasin MD[1]; Chandra Saripalli, MS[1]; John E Smith III, PhD[1]; Carlos G Hidalgo, PhD[1]; Xiuju Luo, MS[1]; Siegfried Labeit, MD[2]; Caiying Guo, PhD[3]; Henk L Granzier, PhD[1] .

[1]Department of Physiology and Sarver Molecular Cardiovascular Research Program, The University of Arizona, Tucson, AZ, USA. [2]Department of Integrative Pathophysiology, Universitätsmedizin Mannheim, University of Heidelberg, Mannheim, Germany [3]HHMI, Janelia Farm Research Campus, Ashburn, VA, USA

*CSC and KRH contributed equally to this study.

CONTENTS

SUPPLEMENTAL METHODS

GENERATION OF MICE EXPRESSING SHORTER TITIN IG SEGMENT

The IG KO was developed as a model of passive stiffness increase that does not remove any known phosphorylation sites[1-3]. The two tandem Ig segments in titin expressed in the dominant N2B isoform are the proximal and distal segments. The proximal Ig domains have a lower stability (reduced unfolding force and increased unfolding rate)[4-7] and we therefore chose to remove these to minimize Ig domain unfolding events in the mutant protein.

Targeting vector construction. The knockout targeting vector was constructed using the recombineering technique described by Liu et al[8]. A 17,778 bp genomic DNA fragment (position chr2:76,734,958 - 76,752,735; Mouse Feb 2006 Assembly) containing exon 19-41 of the gene was retrieved from BAC clone RP23-134B3. A fragment of 6027 bps containing exons 30-38 was replaced by a floxed PGK-neo (PL452) cassette. The 5' homologous arm was 8395 bp and the 3' homologous arm was 3356 bps long.

ES cell targeting and screening. The targeting vector was linearized with Not1 and electroporated into D1 ES cells which were derived from F1 hybrid blastocyst of 129S6 x C57BL/6J by the Gene Targeting & Transgenic Facility at University of Connecticut Health Center. 192 G418 resistant ES colonies were isolated and screened for homologous recombination by nested PCR using primers outside the construct paired with primers inside the neo cassette. Primer sequences were as follows: 5' arm forward primers: TtnIg Scr F1 (5'- TCATGATCCGCGAAGCCTTT -3') and TtnIG Scr F2 (5'- GCACTTCCTGCTATCTTGCT -3'). Reverse primers: Neo scr R1 (5'– GGACGTAAACTCCTCTTCAG -3') and Neo scr R2 (5'- ATGATCGGAATTGGGCTGCA -3'); 3' arm forward primers: Neo scr F3 (5'- TTCTGAGGCGGAAAGAACCA -3') and Neo scr F4, (5'- CGAAGTTATTAGGTCCCTCGA -3'); Reverse primers: TtnIg Scr R3 (5'- TGCAGTTACACCCAGATGAG -3') and TtnIG Scr R4 (5'- TCAGGCACCACTACTGCATT -3'); 6 clones PCR positive for both arms were expanded for generation of chimeric mice.

Chimera generation and mice genotype. The ES cells from two clones (1F5 and 1B9) were aggregated with 8-cell embryos of CD-1 strain. The aggregated embryos were transferred to pseudopregnant recipients and allowed to develop to term. Chimeric mice were identified by coat color and offspring from two chimeras from each line were tested for germline transmission of the targeted allele. The neo cassette was removed by mating the chimeras with a Cre deleter strain (129S1-Hprt$^{tm1(cre)Mnn}$ Stock Number 004302, Jackson Laboratory, Bar Harbor, ME). The F1 pups with neo cassette removed were genotyped by PCR using primer set TtnIg gtF P2 (5'- CACTAGCAGGAACATGTGTC -3') and TtnIg gtR P3 (5'- GCAGCTACCCATATCATAGC -3'). The PCR product is 268 bp for the IG KO allele. Mice were subsequently bred on a C57BL/6 background (Stock Number 000664, Jackson Laboratory) for 8 generations. Template DNA for genotyping was digested from tail tips using Tail Lysis Buffer (0.1mM Tris pH 8.8, 5mM EDTA, 0.2M NaCl, 0.2% SDS) and 0.4 mg/mL proteinase K (Worthington Biochemical Corporation) at 55^{o}C overnight. To discriminate wildtype and knockout alleles, the primers TtnIg gtF P1 (5'- GAACGGTGTGGAGATCAAGT-3') and TtnIg gtR P3 were used for WT and TtnIg gtF P2 and TtnIg gtR P3 were used for the IG KO; the PCR product sizes are 319bp for the WT and 268 bp for the IG KO alleles. The reaction was carried out for 32 cycles (94^{o}C 20s, 55^{o}C 30s and 72^{o}C 30s) followed by one cycle of 72^{o}C for 5 min. 1 µL of the template was amplified using GoTaq Green Master Mix (Promega) in a 20 µL PCR reaction. The heterozygous mice produce litters at Mendelian ratios and breeding was performed with both heterozygous and homozygous (WT/WT or IG KO/IG KO) breeding schemes. Regular backcrossing of homozygous breeders to BL6 lines was performed to eliminate genetic drift.

TITIN GENE EXPRESSION MICROARRAY

We evaluated titin mRNA expression of 3 month old male WT and IG KO hearts using our custom exon microarray as previously described[9]. Briefly, the mouse titin exon probes (50 mer oligonucleotides) were spotted in triplicate on glass slides (Corning Ultra GAPS, Dow Corning, Corning NY). LV lateral wall tissues were dissected and stored in Ambion RNAlater (Invitrogen, Grand Island NY) to preserve RNA. RNA was then isolated using the Qiagen RNeasy Fibrous Tissue Mini Kit (Qiagen, Valencia CA) and amplified using the SenseAmp kit (Genisphere, Hatfield PA) and Superscript III reverse transcriptase enzyme (Invitrogen). Reverse transcription and dye coupling (using Alexa Flour 555 and Alexa Flour 647) was performed using the SuperScript Plus Indirect cDNA Labeling System (Invitrogen) to obtain labeled cDNA. Labeling with Alexa Flours 555 and 647 was alternated between genotypes to eliminate any dye-specific effects. cDNA concentration was evaluated using a Nanodrop system (ThermoScientific, Waltham MA) and 750ng of cDNA from one mouse of each genotype was hybridized on individual slides using SlideHyb Buffer #1 (Ambion) for 16 hours at 42^{o}C after which slides were scanned at 595nm and 685nm with an ArrayWoRx scanner (Applied Precision, Issaquah WA). Spot finding was performed with SoftWoRx Tracker (Applied Precision) and analysis completed in CARMA[10]. CARMA is an analysis package for the R-statistics environment that calculates Loess normalization[10] and detects relative changes in the fluorescence of a probe; these changes are reported as a log-fold-difference that reflects the ratio of IG KO expression per exon vs. WT. A positive fold-change indicates a higher relative expression in the WT, while a negative fold change indicates a decrease (or loss) of expression in the IG KO. A 2-fold change was considered the threshold for differential expression.

QUANTIFICATION OF PROTEIN EXPRESSION

Flash-frozen left ventricular (LV) tissues were prepared as previously described[9, 11, 12]. Briefly, (LV) tissues were snap frozen in liquid nitrogen and solubilized between glass pestles cooled in liquid nitrogen. Tissues were primed at -20^{o}C for a minimum of 20 min, then suspended in 50% urea buffer ([in mol/L] 8 Urea, 2 Thiourea, 0.05 Tris-HCl, 0.075 Dithiothreitol with 3% SDS and 0.03% Bromophenol blue pH 6.8) and 50% glycerol protease inhibitors ([in mmol/L] 0.04 E64, 0.16 Leupeptin and 0.2 PMSF) at 60^{o}C for 10 min, then at room temperature (RT), centrifuged, aliquoted, flash frozen in liquid nitrogen and stored at -80^{o}C.

Titin isoform analysis was performed as previously described[12] with LV samples (n=6) from each genotype at both 3 mo and 12 mo of age. Briefly, solubilized samples were electrophoresed on 1% agarose gels using a vertical SDS-agarose gel system (Hoefer). Gels were run at 15mA per gel for 3 h and 20 min, then stained using Coomassie brilliant blue (Acros organics), scanned using a commercial scanner (Epson 800, Epson Corporation, Long Beach CA) and analyzed using One-Dscan (Scanalytics Inc, Rockville MD). Each sample was loaded in a range of five volumes and the integrated optical density (OD) of titin and MHC were determined as a function of volume. The slope of the linear relationship was obtained for each protein to quantify expression ratios.

Titin phosphorylation levels were quantified via back-phosphorylation assays in LVs from 3 mo WT and IG KO for PKA and western blotting for PKC as previously described[13, 14]. Briefly, to determine PKA phosphorylation levels, fresh left ventricular tissues from WT and IG KO mice (n=5) were obtained and skinned for 24 h in a BES buffered relaxing solution ([in mmol/L] 10 BES, 10 EGTA, 6.56 $MgCl_2$, 5.88 Na-ATP, 1 DTT, 46.35 potassium-propionate, 15 creatine phosphate) with 1% triton X-100 and protease inhibitors ([in mmol/L] 0.1 E64, 0.4 Leupeptin and 0.5 PMSF). LV skinned fibers 2 mm in length, 0.5 mm in diameter were dissected. The fibers were incubated

with 1 U/μL of protein kinase A (PKA) catalytic subunit from bovine heart (Sigma) in a BES buffered relaxing solution. 20 μCi of [γ-^{32}P]ATP stock solution, specific activity 3,000 Ci/mmol (PerkinElmer) were added and the fibers incubated 1 h at RT. The reaction was stopped by adding solubilization buffer (in mol/L: 6 urea, 2 thiourea, 0.058 DTT, 0.0385 Tris HCl, and 2.3% SDS and 0.02% bromophenol blue, pH 6.8). The solubilized samples were electrophoresed on a 2-7% gradient SDS-PAGE, and the gels were subsequently Coomassie blue stained, dried, and exposed to BioMax MS film (Kodak, Rochester NY). The dried gels and the autoradiography films were scanned using an Epson Expression 800 scanner. The images were analyzed with One-Dscan software to obtain the integrated optical density. The titin integrated OD from the autoradiograph was normalized to that of the Coomassie blue stained gels to normalize for protein loading.

For PKC phosphorylation, 6 solubilized samples from both 3 mo old WT and IG KO LVs were run on a 0.8% agarose gel in a vertical gel electrophoresis chamber. Gels run at 15mA per gel for 3 h and 20 min were then transferred onto PVDF membranes (Immobilon-FL, Millipore) using a semi-dry transfer unit (Trans-Blot Cell, Bio-Rad, Hercules CA). Blots were stained with Ponceau S (Sigma) to visualize the total protein transferred and gels were stained with coomassie stain to confirm efficient transfer and both blots and gels scanned to confirm transfer efficiency. Blots were then probed with phosphor-specific rabbit polyclonal antibodies against phosphorylated S26 and S170 of the PEVK element sequence of the titin N2B isoform[13]. Membranes were labeled with secondary antibodies conjugated with fluorescent dyes with infrared excitation spectra (CF680, goat anti-rabbit, Biotium Company, Hayward CA). Blots were scanned using an Odyssey Infrared Imaging System (Li-Cor Biosciences, Lincoln NE) and the images analyzed using Li-Cor software. Ponceau S scans were analyzed in One-Dscan to normalize phosphorylation signal to protein loading.

Myosin isoform analysis was performed using 7% acrylamide gels as previously described[15]. Briefly, 6 solubilized samples from 3 mo and 12 mo old LVs were loaded onto vertical gel electrophoresis chambers with a 4% acrylamide stacking layer and 7% acrylamide resolving layer. Gels were run at 275V for 24 h at 12ºC. Gels were stained with Coomassie brilliant blue because it binds stoichiometrically to proteins, has a wider dynamic range and a wider linear relationship between quantity of protein and staining intensity vs. silver stain. Gels were then scanned and analyzed using One-Dscan software. Each sample was loaded one time, alternating WT and IG KO samples.

Thin and thick filament regulatory proteins expression and phosphorylation were analyzed as previously described[11, 16-18]. Briefly, 5 samples from 3 mo WT and IG KO hearts were loaded on 2-7% gradient SDS-PAGE gels and run using 60V for 1 h followed immediately by running of 90V for 115 min. Gels were fixed in 50% methanol, 10% acetic acid overnight then stained with Pro-Q Diamond Phosphoprotein Gel stain (Invitrogen), destained with 20% acetonitrile, 50 mmol/L sodium acetate pH 4, and scanned with an excitation laser at 532 nm and 560 nm long pass emission filter using a Typhoon 9400 scanner (Amersham Biosciences). Gels were then stained with Coomassie brilliant blue, scanned, and analyzed using One-Dscan for protein content. Each sample was loaded one time, alternating WT and IG KO samples.

Evaluation of titin-based signaling domains was also done using western blotting techniques as previously shown[17]. Solubilized samples from 3 mo and 12mo old WT and IG KO LVs were loaded on 12% SDS-PAGE acrylamide gels and electrophoresed at 100V for 2 h. Gels were then transferred on to PVDF membranes using a semi-dry transfer unit, stained with Ponceau S, scanned, destained and labeled with antibodies to TCap, MLP, FHL1, FHL2, αβ-crystallin, CARP, ANKRD2, MARP3, MURF1 and MURF2 (available from www.myomedix.com) along with GAPDH

or Tubulin (when necessary) for a loading control. Secondary antibodies conjugated with fluorescent dyes with infrared excitation spectra were used and membranes scanned using an Odyssey Infrared Imaging System. Images were analyzed using LiCOR infrared software and normalized either the loading control.

QUANTITATIVE RT-PCR

Total RNA was extracted using the RNeasy Fibrous Tissue Mini Kit with DNase treatment (Qiagen) from left ventricle tissue, which upon dissection had been immediately immersed into RNAlater (Ambion) and stored at -20^{o}C. SuperScript III (Invitrogen) was used to reverse transcribe total RNA for expression studies. RNA quantification and quality assessment were performed using a NanoDrop 1000 Spectrophotometer and a 2100 Bioanalyzer (Agilent); control reactions with 25ng total RNA rather than cDNA (qPCR) were used to confirm that there was no DNA contamination in all samples. Quantitative RT-PCR was performed using a Rotor-gene 6000 (Corbett Life Science) using Maxima SYBR Green qPCR Master Mix (Fermentas) with 60^{o}C annealing temperature. Each reaction included the cDNA equivalent of 25ng total RNA per 20µl reaction. For each gene assayed, standard curves were used to quantify levels from averages of 3 technical replicates for 4 biological replicates from 3 month and 12 month (sedentary) samples. Samples were normalized using standard curves to the *Polr2a, Ppia (Cyclophilin A, CypA), Hprt,* and *Rpl13a* reference genes. The geNorm analysis method was used to select the best normalization (comparing results for all genes tested normalized with every single-gene, double-gene and triple-gene combination -- 14 normalizations total) to identify the Polr2a & Ppia & Rpl13a combination as having the most precise values, minimizing deviation within each group[19, 20]. Specificity of qPCR products was confirmed by melting point analysis; no outliers were removed. Oligonucleotides were synthesized by Integrated DNA Technologies or Invitrogen, sequences are found in Table S4[21-25].

IMMUNOELECTRON MICROSCOPY

Immunoelectron microscopy methods were performed as previously described to estimated segment extension by measuring Z-disk to epitope distances[17, 18, 26]. Briefly, 6 hearts from 6 month old male WT and IG KO mice were quickly excised from heparinized, anesthetized mice, and the LV opened along the septum and pinned to a Sylgard (Dow Corning, Midland MI)-coated petri dish in oxygenated HEPES buffer. Papillary muscles were dissected and placed in an Imidazole buffered relaxing solution ([in mmol/L] 40 Imidazole, 10 EGTA, 6.4 Mg-acetate, 5.9 NaATP, 1 DTT, 70 K-Proprionate, 10 creatine phosphate) with 1% Triton X-100 and protease inhibitors ([in mmol/L] 0.1 E64, 0.4 Leupeptin and 0.5 PMSF) for 24-48 hrs at 4^{o}C with at least one solution exchange. The tissues were washed with Triton-free relaxing buffer for a minimum of 4 hrs (at 4^{o}C). Fibers were microdissected (~150um in diameter, 2mm length), stretched to various lengths from slack up to ~150% of slack length and pinned to a Sylgard coated dish. Tissues were washed with PBS ([in mmol/L] 2.7 KCl, 1.5 KH_2PO_4, 137 NaCl, 8 NaH_2PO_4) and incubated with primary antibodies in PBS for 48 hours at 4^{o}C. Primary antibodies used were: T12, a mouse monoclonal antibody, targeting Ig domains 2-3 (Roche, Indianapolis IN); Un, targeting Ig domains 18-19 and labeling the N-terminal aspect of the N2B unique sequence; Uc, targeting the C-terminal aspect of the N2B unique sequence; I84, Ig-domains 84-86 at the C-terminal side of the PEVK domain (Uc, Un and I84 are rabbit polyclonal antibodies courtesy of Dr. Siegfried Labeit); and I102 an affinity purified polyclonal antibody raised in a rabbit against nucleotide positions 18803-19600 of the Mus musculus titin N2-B cardiac isoform data library entry (GenBank Accession: NM_028004.2, KA Garvey and CC Gregorio, unpublished data). Primary antibodies were labeled in sets using T12, Uc and I102 or Un, I84 and I102 to minimize overlap of epitopes at lower sarcomere lengths. Excess primary antibody was washed from the preparations with fresh PBS for 24 hours, followed by incubation with secondary antibodies for 48

hours at 4°C. Goat anti-Mouse IgG (AP134, Millipore, Billeria MA) and Goat anti-Rabbit IgG (AP 132, Millipore) were co-incubated as secondary antibodies to provide added contrast during electron microscopy imaging. Samples were then washed again with PBS for 24 h and fixed for 20 min using a 3% glutaraldehyde solution, washed in PBS for 24 h to remove unconjugated glutaradelhyde, and incubated with 1%OsO_4 in PBS to post-fix the tissues for 30 minutes. Preparations were finalized after washing with ddH_2O then dehydrated in graded series of ethanol washes (25%, 50%, 75%, 95%, 100%, twice at each step for 15 minutes each). Tissues were then infiltrated with Araldite Epoxy Resin (Araldite 502 Kit, Ted Pella, Redding CA), incubated at 50°C for 2 hours, embedded in a size 3 BEEM capsule (Electron Microscopy Sciences, Hatford PA) and incubated at 60°C for 24-48 hrs. Samples were sliced in a cryotome and adhered to copper square mesh grids. Transmission electron microscopy was performed on a standard TEM system (CM-12 TEM, Phillips). Calibrated images were analyzed using a custom LabView VI (National instruments, Austin TX). Epitope locations were exported and fit using monoexponential curves; epitope separations were estimated via monoexponential fit to obtain sarcomere length dependent segment extensions and deviation estimated as the standard error between mean and epitope locations or distances.

HISTOLOGY

Six hearts each from 3 and 12 month old WT and IG KO mice were obtained and quickly cannulated from anesthetized animals. Hearts were perfused with a calcium free Tyrode solution with 2,3-Butanedione monoxide (BDM) and KCl to maximize relaxation ([in mmol/L] 25 $NaHCO_3$, 30 KCl, 118 NaCl, 1.2 $MgCl_2$, 1.2 NaH_2PO_4, 5 Glucose, 5 Na-Pyruvate, with 5 U/L Insulin and 80 mg/L Bovine Serum Albumin [BSA], 30 BDM). A 4-0 silk suture was advanced through the mitral valve and apex and left in place to eliminate fluid buildup in the ventricle. After 5 minutes, perfusion was rapidly exchanged with a 10% formalin solution (Sigma, St Louis MO) and allowed to perfuse for 10 minutes. These partially fixed hearts were then removed, sliced radially in 4 sections and post-fixed in 10% formalin for 24 hrs. Short-axis cross sections were embedded, sectioned, and stained using Picrosirius Red to quantify collagen content[27]. Stained sections were then imaged on a Zeiss microscope (Imager.M1), and analyzed for collagen content and CSA using custom Axiovision scripts.

SKINNED CELL MECHANICS

Cardiomyocytes were isolated from old male WT and IG KO mice as previously described[17, 28, 29]. Briefly, mice were injected with 100 units heparin IP 10 min prior to isolation. Mice were anesthetized via isoflurane inhalation, sacrificed via cervical dislocation, hearts were rapidly removed, and aorta rapidly cannulated. Langendorff perfusion was begun with a 3mL/min constant flow perfusion using a 37°C calcium free Perfusion Buffer solution ([in mmol/L] 10 HEPES; 113 NaCl, 4.7 KCl, 0.6 KH_2PO_4; 0.6 Na_2HPO_4; 1.2 $MgSO_4$, 12 $NaHCO_3$, 12 $KHCO_3$, 2.5 $MgCl_2$, 5.5 glucose, 10 BDM, and 10 Taurine, with 10 µg/mL Insulin, pH 7.46 at 37°C). After 5 minutes, this calcium free solution was replaced with a digestion solution (Perfusion Buffer with 240U/mg Type II Collagenase (Worthington Biochemical Company, Lakewood, NJ) and 25 µmol/L $CaCl_2$ for activation of the collagenase). Hearts were digested for approximately 10 minutes then washed for 10 minutes with a stop buffer (Perfusion Buffer buffered solution with 0.05 mg/mL bovine calf serum and 7.5 µmol/L $CaCl_2$). Hearts were then removed and placed in a small dish containing calcium free HEPES solution with 20mmol/L BDM and high concentration protease inhibitors ([in mmol/L] 0.1 E64, 0.4 Leupeptin and 0.5 PMSF). The right ventricles and atria were removed, and myocytes were then mechanically dissociated from the LV. Cells were placed in a 15mL tube and allowed to pellet. The supernatant solution was removed and cells resuspended in a BES buffered relaxing solution with 0.3% Triton X-100 (Thermo Scientific, Waltham MA) with a high concentration of protease inhibitors ([in mmol/L] 0.1 E64, 0.4 Leupeptin and 0.5 PMSF). Cells were incubated for 6 minutes then pelleted in a centrifuge at 4°C for 3

minutes at 400 rpm and again washed and resuspended in BES buffered relaxing solution buffer and stored on wet ice.

3-5 myocytes from each isolation were obtained and averaged from 5-6 isolations per genotype for mechanical measurements. For each cell, myocyte suspensions were added to a room-temperature flow-through chamber with relaxing solution, mounted on the stage of an inverted microscope. One end of a single cell was glued to a force transducer (Model 406A or 403A, Aurora Scientific). The free end was then bent with a pulled glass pipette attached to micromanipulator so that the myocyte axis aligned with the microscope optical axis and the cross-sectional area (CSA) was measured. The free end of the cell was released and glued to a high-resolution motor (308B, Aurora Scientific, Aurora, Ontario, Canada). Sarcomere length (SL) was measured using a CCD Camera and IonWizard Software (Ionoptix, Cambridge MA) and slack SL of skinned cells was not different (WT: 1.90 μm and IG KO: 1.89 μm, p=0.9 by Wilcoxon rank sum test). Cells were activated using a pCa 4.5 activating solution ([in mmol/L] 40 BES, 10 $CaCO_3$ EGTA, 6.29 $MgCl_2$, 6.12 Na-ATP, 1 DTT, 45.3 potassium-proprionate, 15 creatine phosphate) and protease inhibitors ([in mmol/L] 0.01 E64, 0.04 Leupeptin and 0.5 PMSF) at sarcomere length 2.0 μm to confirm cell viability and allowed to rest for 15 minutes. All maximal active tensions were >35mN/mm^2 with a statistically significant increase in the IG KO (WT: 47±2 mN/mm^2 (n=7) and IG KO: 58±5 mN/mm^2 (n=90), p=0.04 by Wilcoxon rank-sum test). All mechanical protocols were performed in BES buffered relaxing solution and protease inhibitors at room temperature (24^{o}C).

To measure passive stiffness, cardiomyocytes were stretched from slack length to 2.3 μm, held for 20 seconds, and then released with a ramp speed 1.0 length/sec. All stretch protocols were carried out under sarcomere length control using constant strain rates. Recovery time of at least 7 minutes in between stretches was utilized to prevent memory-effects in subsequent measurements. To further quantify the viscoelastic behavior, sinusoidal oscillations were imposed at SLs of 2.05, 2.1, 2.2 and 2.3 μm using a frequency sweep from 0.1Hz to 100Hz with an amplitude of +/-5% of the cell length. Data was collected using a custom LabVIEW VI (National Instruments, Austin TX) at a sample rate of 1kHz and stored offline.

SKINNED FIBER MECHANICS

Skinned muscle fibers were obtained from 3 month old male WT, and IG KO mice as previously described[17, 18, 29-31]. Briefly, hearts were quickly excised from heparinized, anesthetized mice, and the LV opened along the septum and pinned to a Sylgard (Dow Corning, Midland MI)-coated Petri dish in oxygenated HEPES buffer. Papillary muscles were dissected and placed in a BES buffered relaxing solution with 1% Triton X-100 and protease inhibitors ([in mmol/L] 0.1 E64, 0.4 Leupeptin and 0.5 PMSF) for 24-48 h at 4^{o}C with at least one solution exchange. The tissues were washed with Triton-free relaxing buffer for a minimum of 4 h, infiltrated with a 50% (vol/vol) solution of relaxing solution with protease inhibitors and glycerol for a minimum of 8 h (both at 4^{o}C), and then stored at -20^{o}C. Small fibers (~0.02mm^2 CSA and ~1.0 mm length) were dissected from the papillary muscles and glued at their ends to aluminum clips. Fibers were attached to a force transducer (AE801, SensorOne, Sausalito CA) and length motor (308B Aurora Scientific). Cross sectional area (CSA) was calculated using the dimensions of two perpendicular measurements assuming an ellipsoid shape. To test fiber quality, all preparations were activated at sarcomere length 2.0 μm using a pCa 4.5 solution and achieved tensions of >35 mN/mm^2. The maximum active tensions were reduced in the IG KO, (WT: 47±2 mN/mm^2 (n=17) and IG KO: 42±2 mN/mm^2 (n=18), p=0.02 by Wilcoxon rank sum test). Fibers were washed with relaxing buffer, allowed to rest for 15 min below their slack length, and where then returned to their slack SL. Slack SL was not significantly different (WT: 1.86±0.02 μm and IG KO: 1.90±0.01 μm, p=0.10

by Wilcoxon rank sum test). Mechanical protocols were performed in BES buffered relaxing solution with protease inhibitors ([in mmol/L] 0.01 E64, 0.04 Leupeptin and 0.5 PMSF) at room temperature.

Cardiac muscle fibers were stretched using a stretch-hold-release protocol from their slack sarcomere length to a SL of 2.3 μm at a speed of 1.0 length/sec. The fibers were held at their stretched length for 90 seconds, followed by a release. Myofilaments were extracted using a high KCl concentration (1.0 mol/L) relaxing buffer to depolymerize the thick filaments and high KI concentration (0.6 mol/L) buffer to depolymerize the actin filaments. The stretch-hold-release was then repeated to determine ECM based stiffness. Data was collected from 6 animals per group and stored using a custom LabVIEW VI at a sample rate of 10 kHz and stored offline.

ANALYSIS OF SKINNED MYOCYTE AND MUSCLE MECHANICS

Data was analyzed off line in a custom LabVIEW VI. Stress was calculated by dividing measured force by cross sectional area. The force during the 1.0 length/s stretch was plotted against the sarcomere length and fitted with a monoexponential curve to derive stress-sarcomere length relationships. In cells, the total stiffness was attributed to titin; the slope of the monoexponential curve was calculated in ranges of ±0.5 μm to determine stiffness. In fibers, the stress post myofilament extraction was attributed to the ECM while the difference between the total (pre-extraction stress) and post-extraction stress was attributed to titin[29, 31]. The ECM based stiffness was calculated from 2.0-2.2 μm to overlap the physiologic range in the ex-vivo isolated heart studies.

Frequency sweep data from cells were analyzed to obtain viscous moduli[32]. Briefly, the stress was used to first calculate the complex stiffness as the stress divided by the percent length change. Phase delay was calculated as the phase difference between the stress and strain signals. (For myocyte mechanics, the internal timing/signal processing delay for the force transducer was determined as 12 ms using a glutaraldehyde fixed cell and measured phase was corrected for this delay; no delay was found for the fiber mechanics in the frequency range that was used.) The viscous modulus was then calculated as complex stiffness times the sine of the phase delay. To correct for preparation length, strain was normalized to cell or fiber length.

ISOLATED HEART MECHANICS

Isolated perfused mouse hearts were prepared as previously described[16, 18]. Briefly, WT and IG KO mice were heparinized and anesthetized. Mice were sacrificed (as above) and the hearts quickly cannulated for Langendorff perfusion. Constant pressure (90mmHg) perfusion was provided with an oxygenated 37°C Tyrode solution ([in mmol/L] 25 $NaHCO_3$, 4.7 KCl, 118 NaCl, 1.2 $MgCl_2$, 1.2 NaH_2PO_4, 1.75 $CaCl_2$, 5 Glucose, 5 Na-Pyruvate, with 5 U/L Insulin and 80 mg/L Bovine Serum Albumin [BSA]). Left and right atria were opened for access and the AV-node was heat ablated. A small needle was used to guide a custom plastic balloon in the LV between the mitral valve orifice and LV apex. The balloon was connected to a chamber containing degassed water connected to a servomotor for volume control, and a micromanometric pressure catheter (SPR-471, Millar Instruments, Houston TX). The heart was submerged in a temperature-controlled chamber filled with Tyrode perfusate. Chamber temperature was adjusted to obtain right ventricular chamber (core) temperatures of 37°C. The balloon was inflated to a slightly preloaded volume achieving a diastolic pressure of 5-10 mmHg, and the ventricle was externally paced via field stimulation by platinum electrodes at 500 bpm, typically developing ~75 mmHg developed pressure. The heart was then allowed to equilibrate for approximately 10 minutes. A single beat Frank-Starling protocol was used to probe volumes below baseline (<0mmHg) up to

a volume where maximal developed pressure was resolvable. Frank-Starling protocols were repeated at perfusion pressures of 75, 60, and 45mmHg and returned to 90 mmHg to calculate the pure passive pressure-volume relationship and eliminate turgor effects[16]. Once equilibrated, perfusion was changed to 2 μmol/L dobutamine to maximally stimulate the β-adrenergic pathway. After ~10 minutes of stabilization, the single beat Frank-Starling protocol was repeated. A 2 μmol/L dose of propranolol was also used to block the beta-adrenergic pathway, stabilized and studied via the Frank-Starling protocol. Hearts were then adjusted to one of 3 volume levels (baseline, near the volume of maximal developed pressure, or approximately half way between the two) then fixed in situ for 20 minutes using a 2% glutaraldehyde supplemented Tyrode solution. Hearts were then removed and post fixed for ~24 hrs in the same solution, then washed and stored in phosphate buffered solution (PBS, [in mmol/L] 2.7 KCl, 1.5 KH_2PO_4, 137 NaCl, 8 NaH_2PO_4). After heart removal the single beat Frank-Starling protocol was repeated to determine the elastic properties of the balloon. Volume control and data acquisition was performed using custom PC interface and stored for offline analysis. All data from isolated hearts were analyzed in a custom LabVIEW interface. Pressures were corrected with balloon-measurements at identical volumes with the heart removed.

Pressures were converted to wall stress in order to compare with myocyte and fiber experiments. Typically, spherical models of wall stress have been validated and utilized[18, 33]. However, ventricular geometry is often more elliptical (with the apex to base major axis being longer than the minor axis). Therefore, we compared spherical and elliptical models of wall stress. The equation for a sphere has previously been derived and validated[18, 33]:

$$\sigma_{sphere} = \frac{P}{(1+\frac{1.05*W_{LV}}{V_{LV}})^{2/3}-1} \qquad \text{Eq.S1}$$

where W_{LV} is the ventricular weight calculated by M-mode echocardiography and V_{LV} is the ventricular volume[18]. An idealized elliptical model can be derived in the same method as Eq.S1 by assuming that wall stress is approximately pressure divided by the area of the surrounding band of muscle[33]. Thus, the surrounding muscle area can be calculated using $\pi(r_{epi}^2 - r_{endo}^2)$. Using $V = \frac{4}{3}\pi r^2 l$, for a known volume and length we can calculate:

$$\sigma_{ellipse} = \frac{P}{\frac{3}{4}(\frac{V_{epi}}{l_{epi}} - \frac{V_{endo}}{l_{endo}})} \qquad \text{Eq.S2}$$

where l is length, V_{endo} is the chamber volume, and $V_{epi}=V_{endo}+(1.05*W_{LV})$. In the isolated heart it is relatively simple to calculate spherical wall stress, but elliptical strain requires knowledge of the major (apex to base) length. We measured the major length in post-fixed hearts at known volumes and used this to calculate elliptical wall stress. Stress- volume relationships were significantly different between IGKO and WT for both elliptical and spherical wall stress models with the IG KO showing similar increases for both models (Fig. S3A-D). In the P-V analysis we attempted to get long-axis length from the ultrasound study that was carried out on each mouse prior to the P-V study. However, differences in cardiac parameters between echo and P-V (especially those that are sensitive to anesthesia such as LV volumes, heart rates, etc.) caused too much variability, i.e., the length obtained from echo was unlikely to accurately represent this value in the P-V study. Given the uncertainty in this data and the complexity of its analysis, we elected to use in the main article the validated spherical model to calculate wall stress.[18, 33]. In order to derive the passive pressure-volume and wall-stress volume relationship, the diastolic pressures were corrected for perfusion and turgor effects as previously described[16]. Diastolic stiffness was calculated in the overlapping volume range (~22-28μL). Systolic stress-volume relationships were calculated using the 90mmHg perfusion pressure data at baseline and after dobutamine and propranolol treatment.

To determine stress-sarcomere length relationships, we determined sarcomere lengths as previously described[16]. Briefly, we obtained a transmural section of the lateral free-wall of the heart. Sections were dissected in PBS until circumferential midwall fibers were obtained. Fibers were then placed into custom cut chambers in Sylgard (Dow Corning) coated Petri dishes; chambers were filled with PBS and sealed to prevent a meniscus and eliminate bubbles or evaporation. Sarcomere lengths were measured via laser diffraction and plotted against the volume during fixation to obtain a sarcomere length-volume relationship and a cylindrical model was applied via a square-root relationship. (Linear, quadratic and quartic (spherical model) relationships had minimal differences in this volume range. Since apex-base length was not significantly different (data not shown), a quadratic (square-root) relationship was used.) The relationship was fit for the IG KO and WT hearts separately and volumes converted to sarcomere lengths. This relationship was used to convert stress-volume relationships to stress-sarcomere length relationships. Stiffness was calculated in the physiologic sarcomere length range (2.0-2.3 μm).

EXERCISE TOLERANCE

Maximal and voluntary exercise tolerance testing was performed on 6 mice per genotype. Maximal exercise testing was performed using a 6-lane rodent treadmill system (Exer 3/6, Columbus Instruments, Columbus, OH). Exercise testing was performed at a 25% incline and having mice run at progressively increasing speeds (speed steps of 5 m/min). Mice ran for 160 s with a 50 s rest period between running periods, after which the protocol was repeated but at a 5 m/min greater speed. Maximal Tolerance was determined when the mouse left the treadmill and remained on a shock pad for 5 s. Tolerance was scored according to the speed of the last completed running period plus the fractional duration of the period before fatigue times 5 m/min (score=completed running period speed+5x pre-fatigue duration of final protocol /160s). Volunteer exercise tolerance was measured in 3 mo and 12 mo old animals[34]. Briefly. Individual animals were housed in a large cage that contained a free wheel for 21 days. The exercise wheels have been previously described[34]. Briefly, an 11.5cm-diameter wheel with a 5.0cm wide running surface (6208; PetSmart; Phoenix, AZ) was equipped with a digital magnetic counter (BC600, Sigma Sport, Olney Il) that is activated by wheel rotation. All animals were given water and standard rodent feed ad libitum. Daily exercise values for time and distance run were recorded.

IN-VIVO PRESSURE VOLUME RELATIONSHIPS

In-vivo pressure volume analysis was performed in mice using a SciSense Advantage Admittance Derived Volume Measurement System and 1.2f catheters with 4.5 mm electrode spacing (SciSense, London, Ontario, Canada). Mice were anesthetized and ventilated with 1% isoflurane using an SAR-1000 Ventilator (CWE Inc) and body temperature maintained at 37^{o}C using a TC-1000 Temperature Controller (CWE Inc). Three mo old anesthetized mice were secured and a mid-line incision was made down the neck. The muscles in the neck were separated and the right carotid artery was isolated from the vagus nerve. The right carotid artery was cannulated and the catheter guided past the aortic valve. The abdomen was opened below the sternum; the IVC was located and occluded during a sigh (pause) in ventilation to find load-independent indexes.

Data acquisition and preliminary analysis was performed in LabScribe2 (iWorx, Dover NH). End diastolic pressure-volume data was exported to MS Excel (Microsoft Corporation, Redmond WA) and a custom LabView VI where end diastolic and end systolic wall stress were calculated. Pressures were converted to wall stress using a spherical model as in Eq.S1. The spherical model provided a conservative estimate of wall stress without requiring values of ventricular lengths, which could not be measured simultaneously with PV measurements (the use of non-simultaneous measurements of major-axis length introduces a major source of error in the

calculation). PV data on 3 mo old mice, acquired via the carotid approach, was fit to linear PV and stress-volume curves with linear slopes reported as the stiffness (EDPVR). (Monoexponential fits did not converge on a unique parameter set.) The PV data on 12 mo old mice was acquired via apical stab (see above) and this type of data made it possible to fit stress-volume data using a monoexponential fit ($P = Ae^{\beta V}$)[35] with the exponent (β) reported as the stiffness.

IN-VIVO ECHOCARDIOGRAPHY

Echocardiographic data was acquired on 12 mo WT and IG KO mice after 21 days of volunteer exercise tolerance using a Vevo 770 small animal echocardiography imaging system (VisualSonics, Toronto, Ontario). Briefly, chest hair was removed and mice were consciously echoed while scruffing the skin at the nape of the neck and a standard short axis (M-mode) cine loop was recorded at the level of the papillary muscles to asses chamber dimensions (LV systolic and diastolic dimensions (LVDs, LVDd)) posterior wall thickness (PWT) and cardiac function via fractional shortening (%FS). Left atrial dimensions were obtained from m-mode acquisition in parasternal long axis (PLA) view in conscious mice. Mice were subsequently anesthetized under a 1% isoflurane/oxygen mixture and secured to a temperature controlled scan table. Following anesthesia the 4-chamber view was used to obtain cardiac diastolic function (E-wave, A-wave, Tissue Doppler). Data was analyzed in Vevo770 3.0 software suite (Visualsonics).

SINGLE MOLECULE MODELING.

The force-SL relations were calculated using the wormlike chain (WLC) equation[36] with three serially-linked WLCs, representing the combined tandem Ig segments, the PEVK, and N2B-Us spring elements[37]. We assumed a contour length (CL) of tandem Ig segments of 200 nm (40 Ig domains with an average spacing of 5 nm) in WT N2B cardiac titin and 155 nm in the IG KO (31 Ig domains with an average spacing of 5 nm). The PEVK contour length was assumed to be of 70 nm and the N2B Us CL 200 nm. The assumed persistence lengths (PL) were 12 nm, 1.0 nm and 0.65 nm, respectively. (For experimental evidence that underlies these values and additional details, see [17, 26, 37, 38].) We then calculated the force-SL relation of a single titin molecule and compared results for WT with IG KO, along the values obtained for N2B KO and PEVK KO molecules (calculated by setting the CL of N2B element/PEVK element to zero). From the obtained force values the stress ration was calculated between the IG KO and WT molecules.

STATISTICS

Non-parametric Mann-Whitney (Wilcoxon sign rank) tests were used to determine significant differences. Analysis was performed in SAS 9.3 (SAS Institute, Cary NC) or MS Excel 2010 (Microsoft Corporation, Redmond WA). Results are shown as mean ± SEM, with $p<0.05$ taken as significant.

Isolated Heart Analysis	WT	IG KO
Baseline LV Volume [µL]	23.5 ± 0.4	21.6 ± 0.4 **
Developed LV Stress (max) [mmHg]	45.9 ± 3.1	54.1 ± 4.3
dP/dtmax [mmHg/ms]	1.66 ± 0.07	2.04 ± 0.10 *
dP/dtmin [mmHg/ms]	-0.94 ± 0.05	-0.98 ± 0.05
Tau [ms]	-41.6 ± 3.0	-38.9 ± 1.9
SSVR [mmHg/µL]	2.68 ± 1.40	4.33 ± 0.94 **
DSVR [mmHg/µL]	2.19 ± 0.38	3.90 ± 0.66 *

In-vivo Pressure Volume Analysis	WT	IG KO
HR [bpm]	572.3 ± 9.8	565.8 ± 22.2
ESP [mmHg]	100.9 ± 2.1	102.2 ± 3.4
EDP [mmHg]	4.2 ± 0.5	5.1 ± 1.0
dP/dtmax [mmHg/s]	12,090 ± 440	11,600 ± 380
dP/dtmin [mmHg/s]	-10,210 ± 300	-10,260 ± 390
ESV [µL]	25.8 ± 1.8	25.0 ± 1.8
EDV [µL]	57.2 ± 1.9	55.0 ± 1.7
SV [µL]	31.4 ± 2.1	29.9 ± 2.2
EF [%]	54.8 ± 2.8	54.1 ± 3.5
SW [mmHg µL]	0.448 ± 0.025	0.401 ± 0.021
Tau (Glantz) [ms]	7.03 ± 0.55	6.96 ± 0.70
ESSVR [mmHg/µL]	3.35 ± 0.10	3.76 ± 0.26
EDSVR [mmHg/µL]	0.14 ± 0.01	0.19 ± 0.02 *

Table S1. Left ventricular properties derived from Isolated Mouse Heart (n=12) and In-vivo Pressure Volume (n=10) analysis at 3 mo. Data shown as mean±SEM. Abbreviations: dP/dtmax: maximum rate of pressure increase during contraction; dP/dtmin: minimum rate of pressure decrease during relaxation; tau: time constant of isovolumic relaxation; SSVR: systolic stress-volume relationship; DSVR: diastolic stress volume relationship; HR: heart rate; ESP: end systolic pressure; EDP: end diastolic pressure; ESV: end systolic volume; EDV: end diastolic volume; EF: ejection fraction; SW: stroke work; ESSVR: end systolic stress volume relationship; end diastolic stress volume relationship. * $p<0.05$; ** $p<0.01$.

	3mo		12mo	
	WT	**IG KO**	**WT**	**IG KO**
HW [mg]	123.5 ± 2.3	112.8 ± 2.5	139.1 ± 2.4	151.8 ± 7.3 *
LVW [mg]	92.4 ± 1.5	83.3 ± 1.4 ***	101.5 ± 1.9	111.0 ± 4.7*
RVW [mg]	24.5 ± 0.6	24.8 ± 1.4	28.8 ± 0.6	29.9 ± 1.5
LAW [mg]	3.90 ± 0.14	4.07 ± 0.18	4.50 ± 0.22	4.68 ± 0.26
RAW [mg]	3.80 ± 0.22	3.90 ± 0.29	4.84 ± 0.20	4.57 ± 0.24
Lung W [mg]	148 ± 3	138 ± 3 *	172 ± 7	171 ± 10
BW [g]	26.9 ± 0.3	23.8 ± 0.2 ***	39.7 ± 0.8	28.6 ± 0.8 ***
HW:BW [mg/g]	4.7 ± 0.1	4.7 ± 0.1	3.6 ± 0.1	5.3 ± 0.2 ***
LVW:BW [mg/g]	3.5 ± 0.1	3.5 ± 0.0	2.6 ± 0.1	4.0 ± 0.1 ***
RVW:BW [mg/g]	0.92 ± 0.01	1.01 ± 0.03 **	0.73 ± 0.02	1.07 ± 0.06 **
LAW:BW [mg/g]	0.14 ± 0.01	0.16 ± 0.01	0.11 ± 0.01	0.16 ± 0.01
RAW:BW [mg/g]	0.14 ± 0.01	0.16 ± 0.01	0.12 ± 0.01	0.16 ± 0.01
Lung W:BW [mg/g]	5.6 ± 0.1	5.9 ± 0.1 *	4.4 ± 0.2	6.1 ± 0.4 ***
Tibial L [mm]	17.8 ± 0.1	17.7 ± 0.1	18.3 ± 0.1	18.2 ± 0.1
HW:Tibial L [mg/mm]	7.07 ± 0.18	6.83 ± 0.18	7.64 ± 0.13	8.37 ± 0.41 *
LVW:Tibia L [mg/mm]	5.12 ± 0.13	4.85 ± 0.11	5.57 ± 0.10	6.14 ± 0.25 **
RVW:Tibia L [mg/mm]	1.41 ± 0.04	1.54 ± 0.15	1.58 ± 0.04	1.66 ± 0.08
LAW:Tibia L [mg/mm]	0.23 ± 0.01	0.25 ± 0.01	0.25 ± 0.01	0.26 ± 0.01
RAW:Tibia L [mg/mm]	0.22 ± 0.01	0.24 ± 0.02	0.26 ± 0.01	0.25 ± 0.01
Lung W: Tibial L [mg/mm]	8.5 ± 0.2	8.0 ± 0.2	9.4 ± 0.4	9.4 ± 0.5

	3mo		12mo	
Protein Expression	**WT**	**IG KO**	**WT**	**IG KO**
N2B:N2BA	0.27 ± 0.02	0.29 ± 0.01	0.29 ± 0.02	0.26 ± 0.01
T2:T1	0.14 ± 0.02	0.16 ± 0.02	0.16 ± 0.01	0.16 ± 0.02
TT:MHC	0.19 ± 0.01	0.19 ± 0.01	0.22 ± 0.01	0.22 ± 0.01
βMHC/αMHC ratio	0.0044 ± 0.0006	0.0044 ± 0.0006	0.020 ± 0.008	0.014 ± 0.004

Table S2. **Comparison of body weight, cardiac mass, protein expression and gene expression at 3 and 12 months of age.** Data shown as mean±SEM. BW: body weight; HW: whole heart weight; LVW: left ventricular weight; RVW: right ventricular weight; LAW: left atrial weight: RAW: right atrial weight; tibial L: tibia length; N2B: short cardiac titin isoform; N2BA: long cardiac titin isoform; T2:T1: ratio of degraded to intact titin; TT:MHC: ratio of total titin protein to myosin heavy chain. Data based on the following n-numbers: for 3 mo: n>20 cardiac weights and tibia lengths, n>80 for BW; for 12 mo: n>8 cardiac weights and tibia lengths, n>15 for BW; n=6 for protein expression. * p<0.05; **p<0.01; ***p<0.001 for IG KO vs. WT per age group.

	WT	IG KO
BW [g]	38.0 ± 1.6	34.5 ± 2.0
Tibia L [mm]	18.6 ± 0.1	18.4 ± 0.1
LA W [mg]	4.97 ± 0.41	6.87 ± 0.47**
LA W:Tibia L [mg:mm]	0.27 ± 0.02	0.37 ± 0.03**
Exercise Tolerance		
Distance [km/day]	4.1 ± 0.9	2.1 ± 0.4 *
In vivo Pressure Volume Analysis		
HR [bpm]	533 ± 23	539 ± 12
ESP [mmHg]	104 ± 5	97 ± 4
EDP [mmHg]	3.7 ± 0.5	3.8 ± 0.3
dP/dtmax [mmHg/s]	11,400 ± 900	10,100 ± 700
dP/dtmin [mmHg/s]	-9,900 ± 500	-10,300 ± 600
ESV [µL]	22 ± 4	27 ± 4
EDV [µL]	58 ± 3	61 ± 3
SV [µL]	36 ± 2	34 ± 2
EF [%]	62 ± 5	56 ± 4
SW [mmHg µL]	0.46 ± 0.02	0.41 ± 0.02
Tau (Glantz) [ms]	8.9 ± 0.9	7.5 ± 0.5
EDPVR (β) [mmHg/µL]	0.048 ± 0.002	0.068 ± 0.006 **
EDSVR (β) [mmHg/µL]	0.060 ± 0.001	0.081 ± 0.005 **
ESPVR [mmHg/µL]	6.9 ± 0.8	6.3 ± 1.1
ESSVR [mmHg/µL]	4.2 ± 0.4	4.5 ± 0.5
Echocardiography		
FS [%]	47 ± 2	44 ± 2
MV DT	28.4 ± 1.0	26.2 ± 0.5
E/A	1.3 ± 0.1	1.5 ± 0.1
LA Dimension [mm]	2.2 ± 0.1	2.8 ± 0.1 ***

Table S3. **Exercise tolerance and cardiac function in 12 mo mice after 21 days of volunteer exercise.** Abbreviations: BW: body weight; Tibia L: tibia length; LA W: left atrial weight;HR: heart rate; ESP: end systolic pressure; EDP: end diastolic pressure; dP/dtmax: maximum rate of pressure increase during contraction; dP/dtmin: minimum rate of pressure decrease during relaxation; ESV: end systolic volume; EDV: end diastolic volume; SV: stroke volume; EF: ejection fraction; SW: stroke work; tau: time constant of isovolumic relaxation; EDPVR (β): monoexponential fit derived end diastolic pressure-volume relationship; EDSVR (β): monoexponential fit derived end diastolic (spherical) wall stress-volume relationship; ESPVR: end systolic pressure-volume relationship; ESSVR: end systolic (spherical) wall stress-volume relationship; FS: fractional shortening; MV DT; mitral valve deceleration time; E/A: mitral valve peak E-wave to A-wave velocity ratio; LA: left atrium. Data shown as mean±SEM, n=6 * $p<0.05$; ** $p<0.01$.***$p<0.001$.

Gene	NCBI geneID	Forward Primer	Reverse Primer	Product Size (bp)	Ref
Polr2a	20020	5'-TCAAGAGAGTGCAGTTCGGA-3'	5'-GGATCCATTAGTCCCCCAAG-3'	127	[24]
Ppia (cyclophilin A)	268373	5'-CAGACGCCACTGTCGCTTT-3'	5'-TGTCTTTGGAACTTTGTCTGCAA-3'	133	[22]
Hprt	15452	5'-TCCTCCTCAGACCGCTTTT-3'	5'-CATAACCTGGTTCATCATCGC-3'	95	[24]
Rpl13a	22121	5'-GGCTGAAGCCTACCAGAAAG-3'	5'-TTCTCCTCCAGAGTGGCTGT-3'	94	[24]
Nppa (ANP)	230899	5'-ATTGACAGGATTGGAGCCCAGAGT-3'	5'-TGACACACCACAAGGGCTTAGGAT-3'	133	DIH
Nppb (BNP)	18158	5'-ACAAGATAGACCGGATCGGA-3'	5'-ACCCAGGCAGAGTCAGAAAC-3'	110	[24]
Mapkapk2	17164	5'-GTGTGGGTATCCCCCCTTCT -3'	5'-TACGAGTCTTCATGCCCGG-3'	65	[23]
Myh6 (αMHC)	17888	5'-CCGGGTGATCTTCCAGCTAA-3'	5'-GCTCAGCACATCAAAGGCACT-3'	208	[25]
Myh7 (βMHC)	140781	5'-TCCCAAGGAGAGACGACTGTG-3'	5'-CCTTAAGCAGGTCGGCTGAGT-3'	253	[25]
Acta1 (Skeletal actin)	11459	5'-GCCGTTGTCACACACAAGAG-3'	5'-CTCACTTCCTACCCTCGGC-3'	102	[24]
Ppp3ca (calcineurin)	19055	5'-GGGACATCCATGGACAATTC-3'	5'-AAGGCCCACAAATACAGCAC-3'	142	[21]
NFATc1	18018	5'-CCCGTTGCTTCCAGAAAATA-3'	5'-TCACCCTGGTGTTCTTCCTC-3'	125	DIH
NFATc2.a (isoform a)	18019 (NM_010899)	5'-CGACGCCTTCTACTCTGGAC-3'	5'-CCATGGACAACGGCTAAGAT-3'	141	DIH
NFATc2.c (isoform c)	18019 (NM_001037178)	5'-CTTTATTGCCTCTCCCACCA-3'	5'-TCCAGATCTTTCCCCAGTTG-3'	122	DIH
Rcan1.4 (calcipressin isoform2)	54720 (NM_019466.3)	5'-CCCGTGAAAAAGCAGAATGC-3'	5'-TCCTTGTCATATGTTCTGAAGAGGG-3'	141	[22]
Col1a1	12842	5'-ACATGTTCAGCTTTGTGGACC-3'	5'-TAGGCCATTGTGTATGCAGC-3'	110	[24]
Col1a2	12843	5'-AAGGAGTTTCATCTGGCCCT-3'	5'-AGCAGGTCCTTGGAAACCTT-3'	101	[24]
Col3a1	12825	5'-GGAACCTGGTTTCTTCTCACC-3'	5'-TAGGACTGACCAAGGTGGCT-3'	98	[24]
MMP13	17386	5'-TGATGAAACCTGGACAAGCA-3'	5'-GGTCCTTGGAGTGATCCAGA-3'	98	[24]
MMP2	17390	5'-CCAGCAAGTAGATGCTGCCT-3'	5'-GGGGTCCATTTTCTTCTTCA-3'	106	[24]
TIMP2	21858	5'-CGTTTTGCAATGCAGACGTA-3'	5'-GAATCCTCTTGATGGGGTTG-3'	99	[24]
TIMP4	110595	5'-ACACGCCATTTGACTCTTCC-3'	5'-CCCAGGGCTCAATGTAGTTG-3'	132	[24]
Lox	16948	5'-GGAGGACACGTCCTGTGACT-3'	5'-CTATGTCTGCCGCATAGGTG-3'	104	[24]

Table S4. Primers used in qPCR. Ref: see Supplemental References, pg. 21; DIH: designed in house.

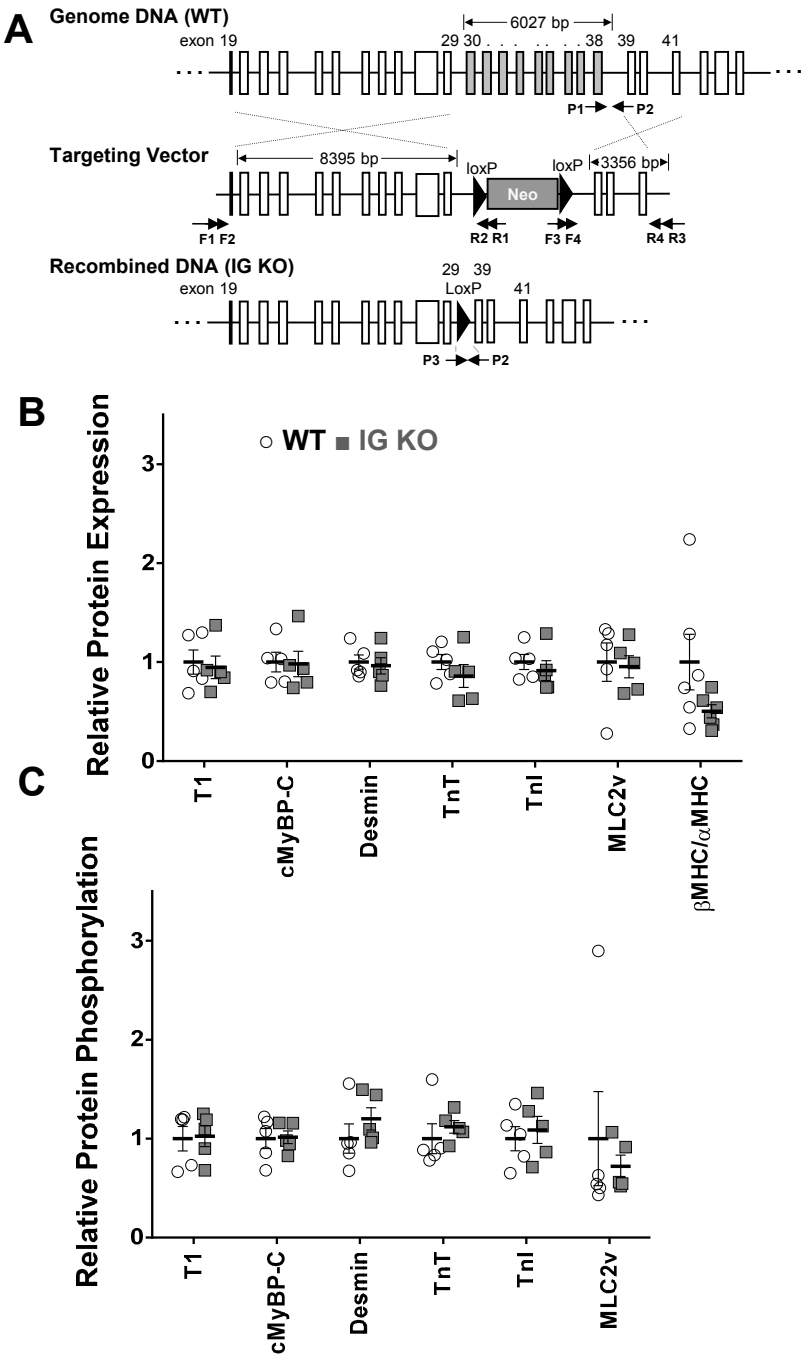

Figure S1. Generation and basic characterization of the IG KO mouse model. A) targeting strategy for gene KO of titin exons 30-38 that encode Ig 3-11. Genotyping (P) and screening (F,P) primers are shown as described in the supplementary methods. Comparison of 3 mo old WT and IG KO cardiac sarcomeric protein expression (B) and phosphorylation (C) of sarcomeric protein relative to WT at 3 months of age. Horizontal lines denote mean±SEM, n=5. No significant differences were detected.

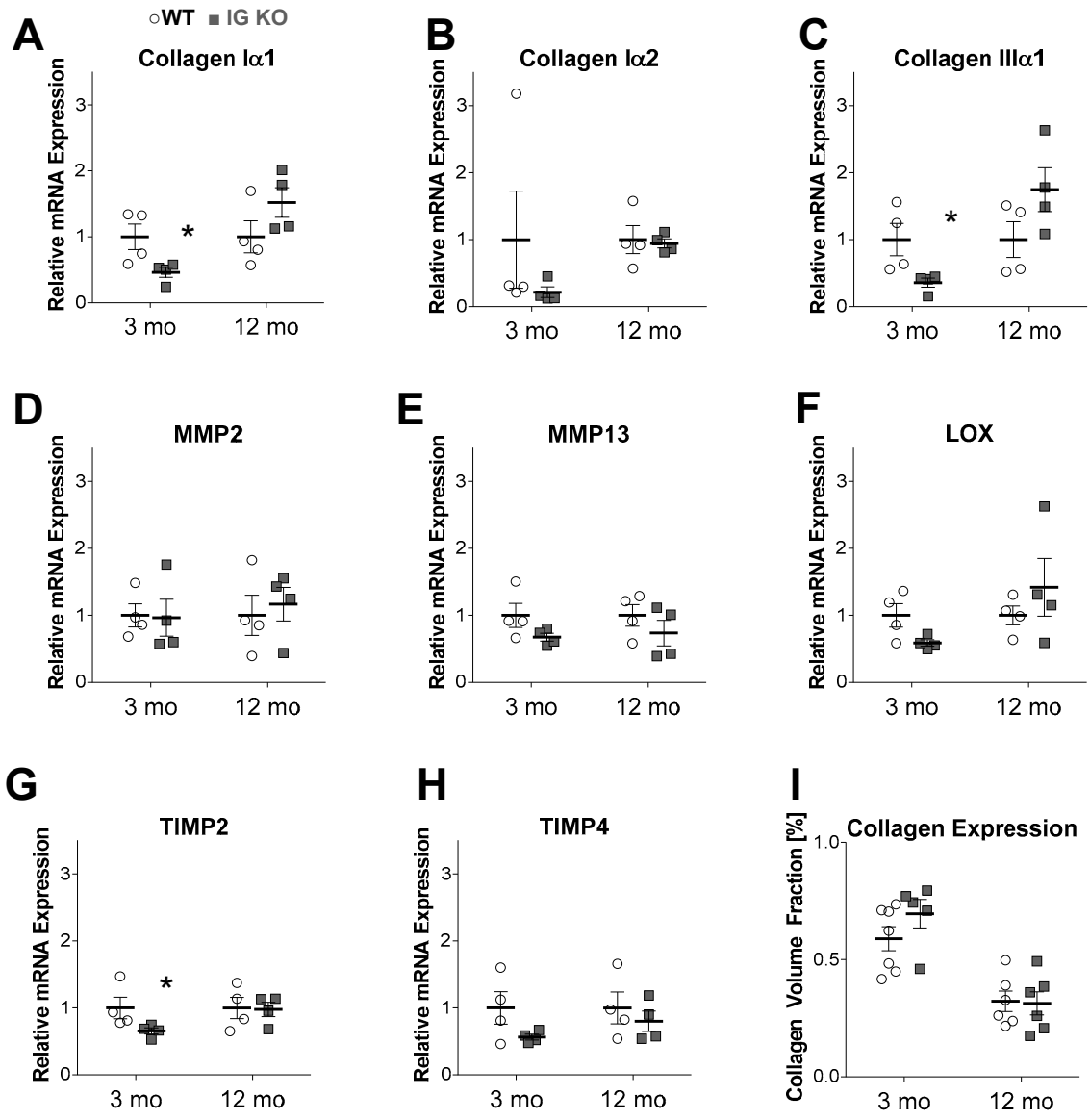

Figure S2. Expression of ECM-components in sedentary 3 and 12 mo old WT and IG KO mice. Panels A-H, qPCR data normalized to WT per age group and shown as mean±SEM (n=4). Panel I, Picrosirius Red staining (n=5). Horizontal lines denote mean±SEM, * $p<0.05$ for IG KO vs. WT per age group.

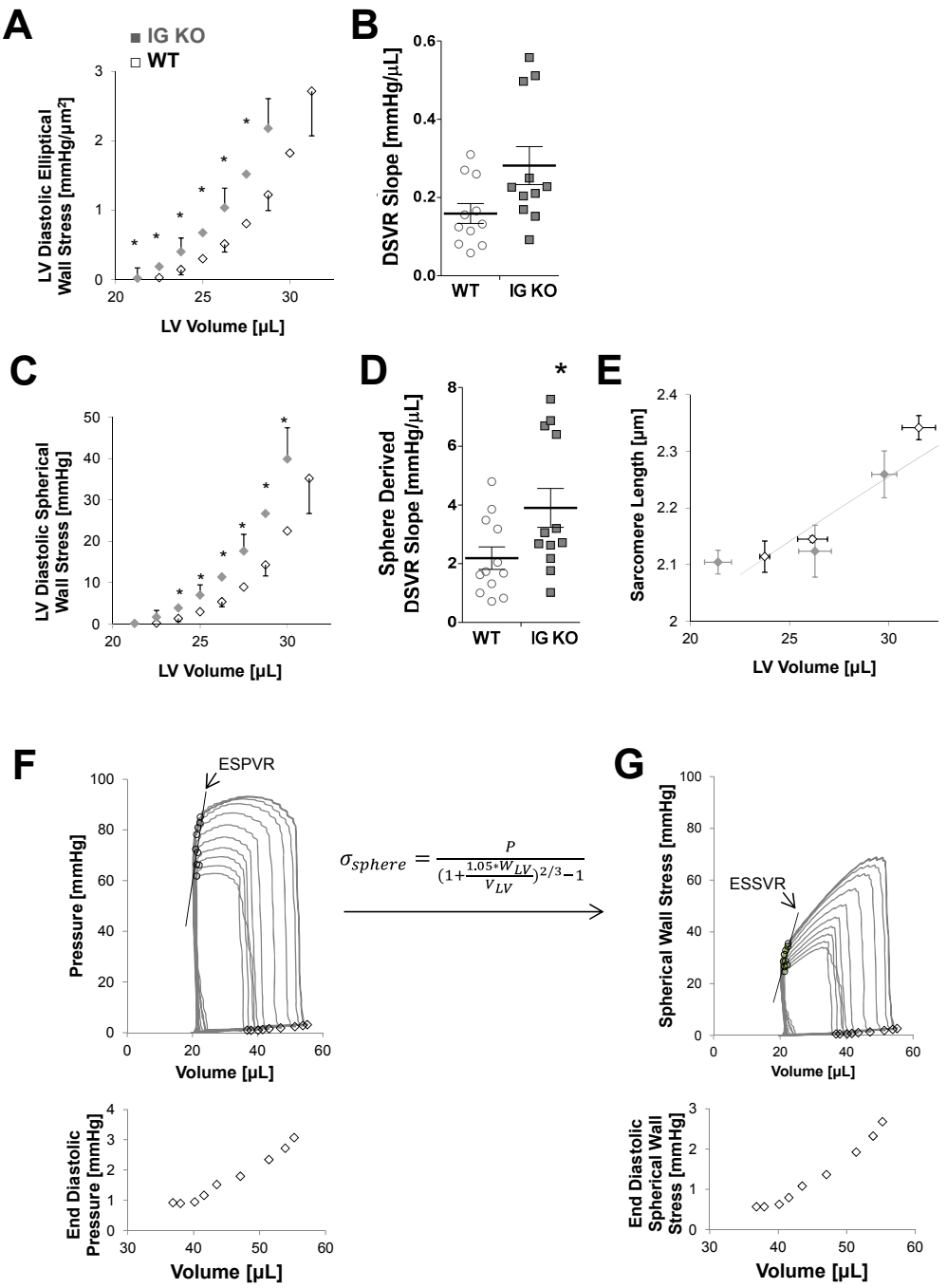

Figure S3. Wall Stress, sarcomere length and pressure-volume relationships. Elliptical (A,B) and spherical models (C,D) of wall stress of isolated hearts show in IG KO mice similar relative increases in diastolic stiffness of DSVR relationships. (n=12). After fixing hearts at specific preload, the sarcomere length volume relationship was determined (E) (n=4 per group per volume). Example in-vivo PV from a 3mo IG KO mouse (F) and stress-volume (G) relationships (top: full IVC occlusion, line shows end systolic P-V relationship; bottom: data for end diastolic relationships). Horizontal lines denote mean±SEM, * p<0.05.

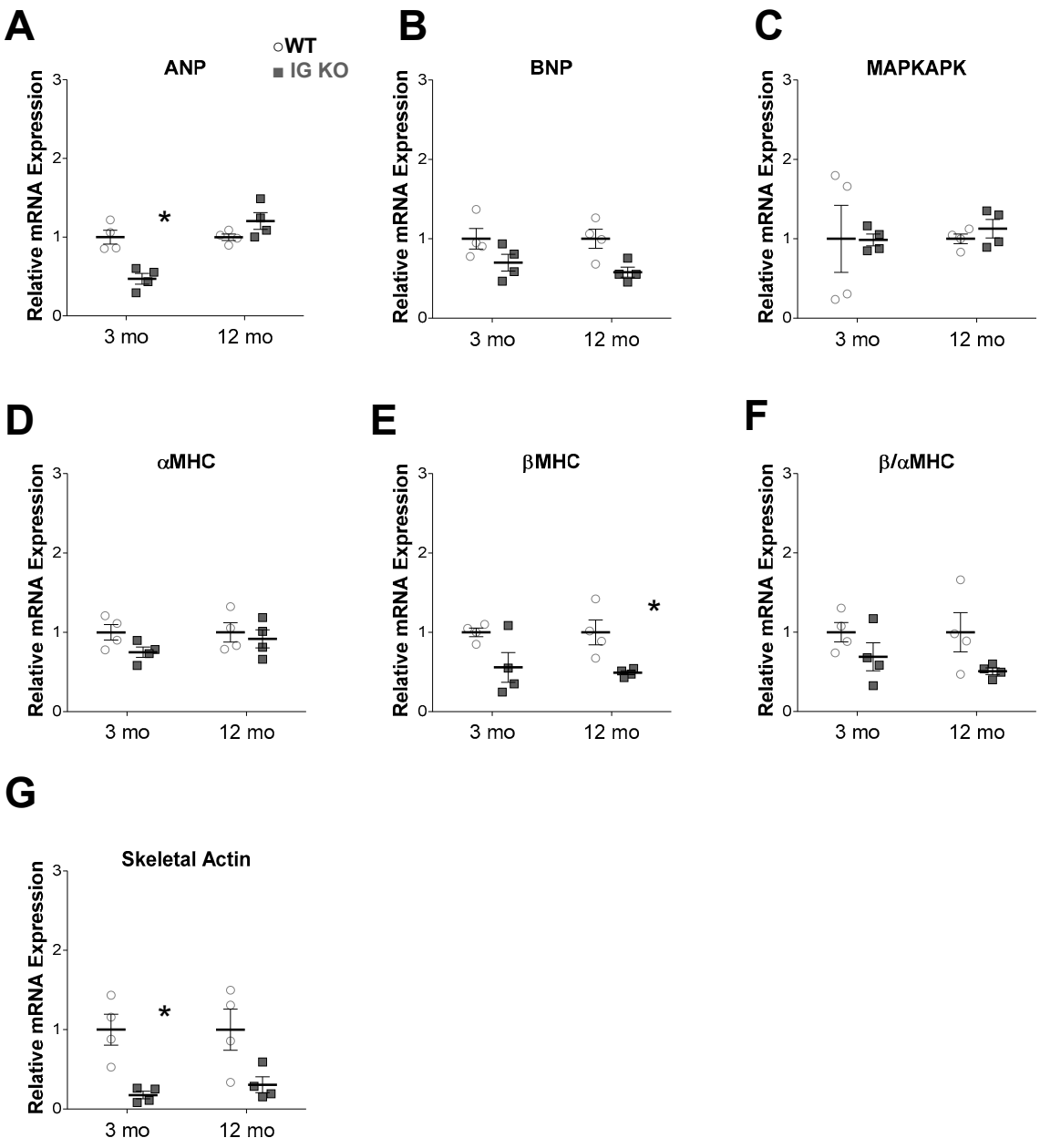

Figure S4. Markers for cardiac disease and failure. Atrial natriuretic peptide (A, ANP), b-type natriuretic peptide (B, BNP), MAPKAPK2 (C), and myosin heavy chain isoform expression and expression ratios (D-F) and skeletal actin (G) are shown. Data normalized to WT per age group and shown as mean±SEM, n=4. Horizontal lines denote mean±SEM, * $p<0.05$ for IG KO vs. WT per age group.

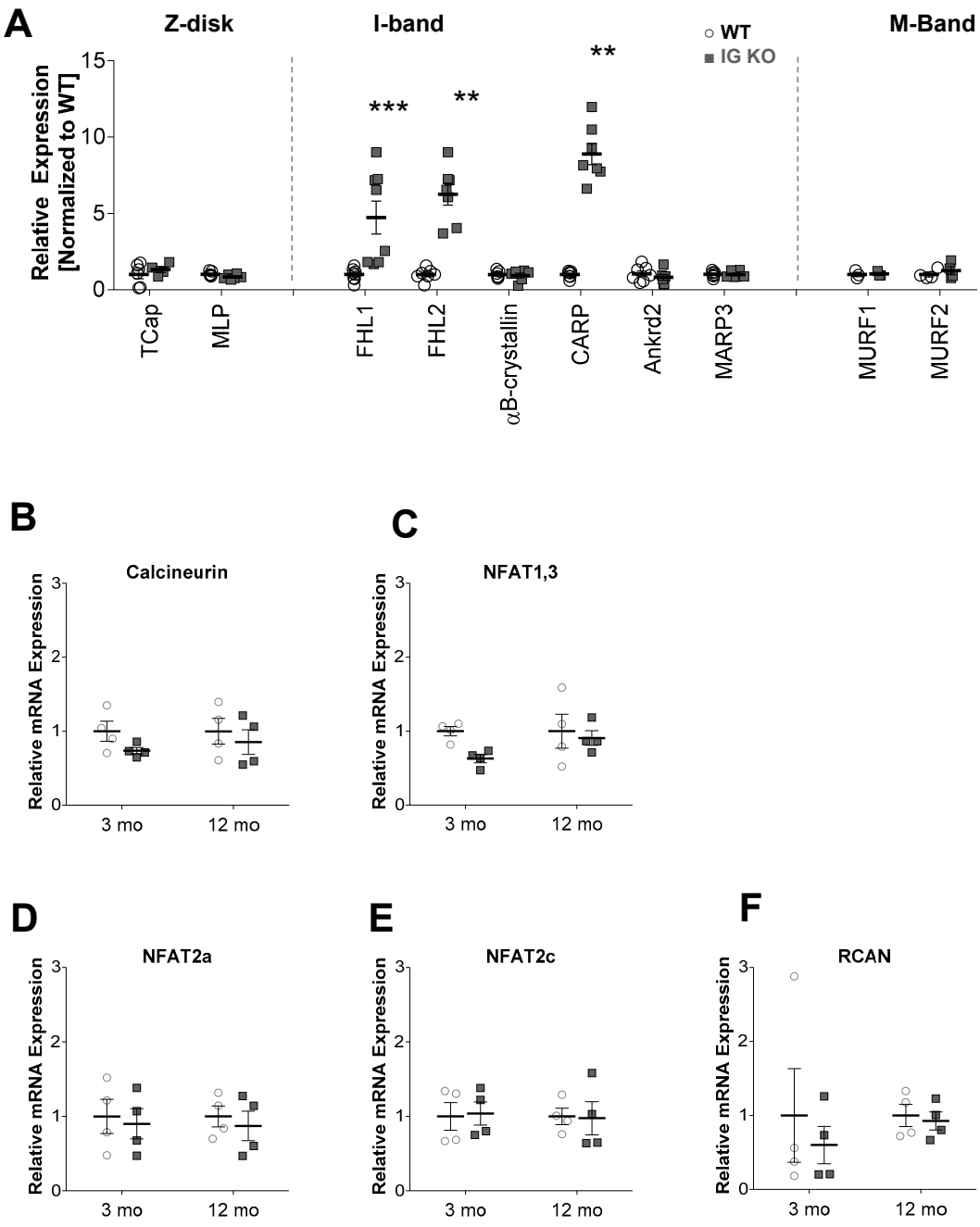

Figure S5. Expression of titin binding proteins (A) and calcineurin hypertrophic pathway markers (B-F) . Expression of titin-binding proteins is unaltered except for the I-band binding proteins FHL1, FHL2, and CARP (A). Calcineurin (B) and NFAT (C-E) mRNA expression are also unchanged along with the primary downstream marker of the calcineurin hypertrophy pathway RCAN1,4 (F). Data normalized to WT per age group; horizontal lines denote mean±SEM, n=4. ** p<0.01.***p<0.001 for IG KO vs. WT per age group.

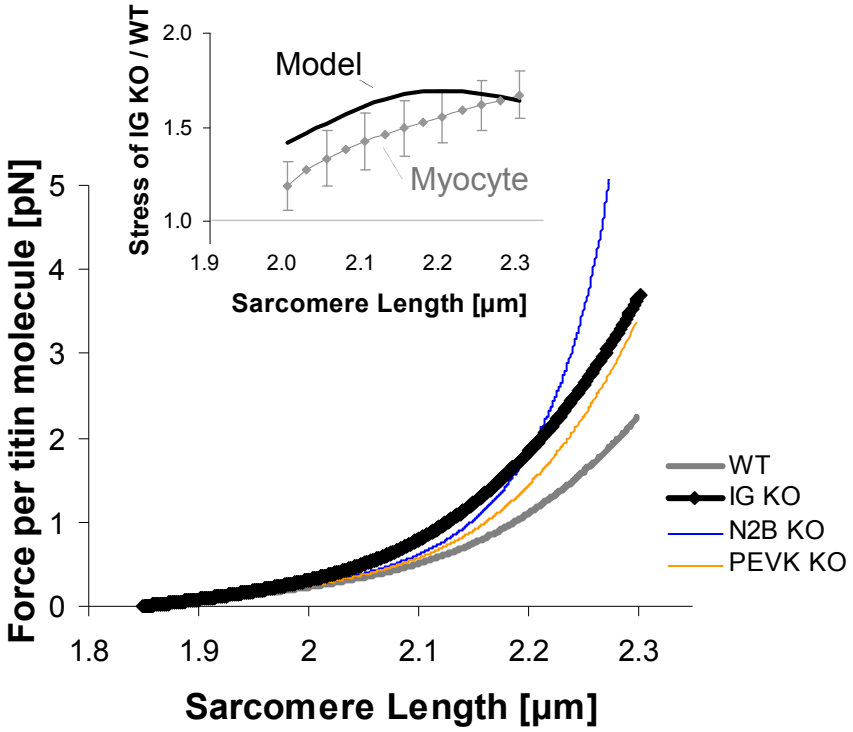

Figure S6. Single molecule modeling. A) Predicted force-SL relationship of single titin molecule (N2B cardiac titin isoform). WT (gray) and IG KO molecules (thick black). Orange line is predicted force of PEVK KO molecule and blue line of N2B KO molecules. At SLs <~2.2 µm force is highest in the IG KO and only towards the upper limit of the physiological SL range the values in the N2B KO and PEVK KO models exceed those in the IG KO. The large increases in the IG KO model at short to intermediate SLs can be explained by the previous findings that tandem Ig segments dominate titin extension at short to intermediate SL (due to their long persistence length[38]). Inset shows the fractional increase in stress of the IG KO vs. WT from model data (thick black line) and from the cardiomyocyte data (gray line, error bars denote SE; data from Fig.2A). For details, see Supplemental methods.

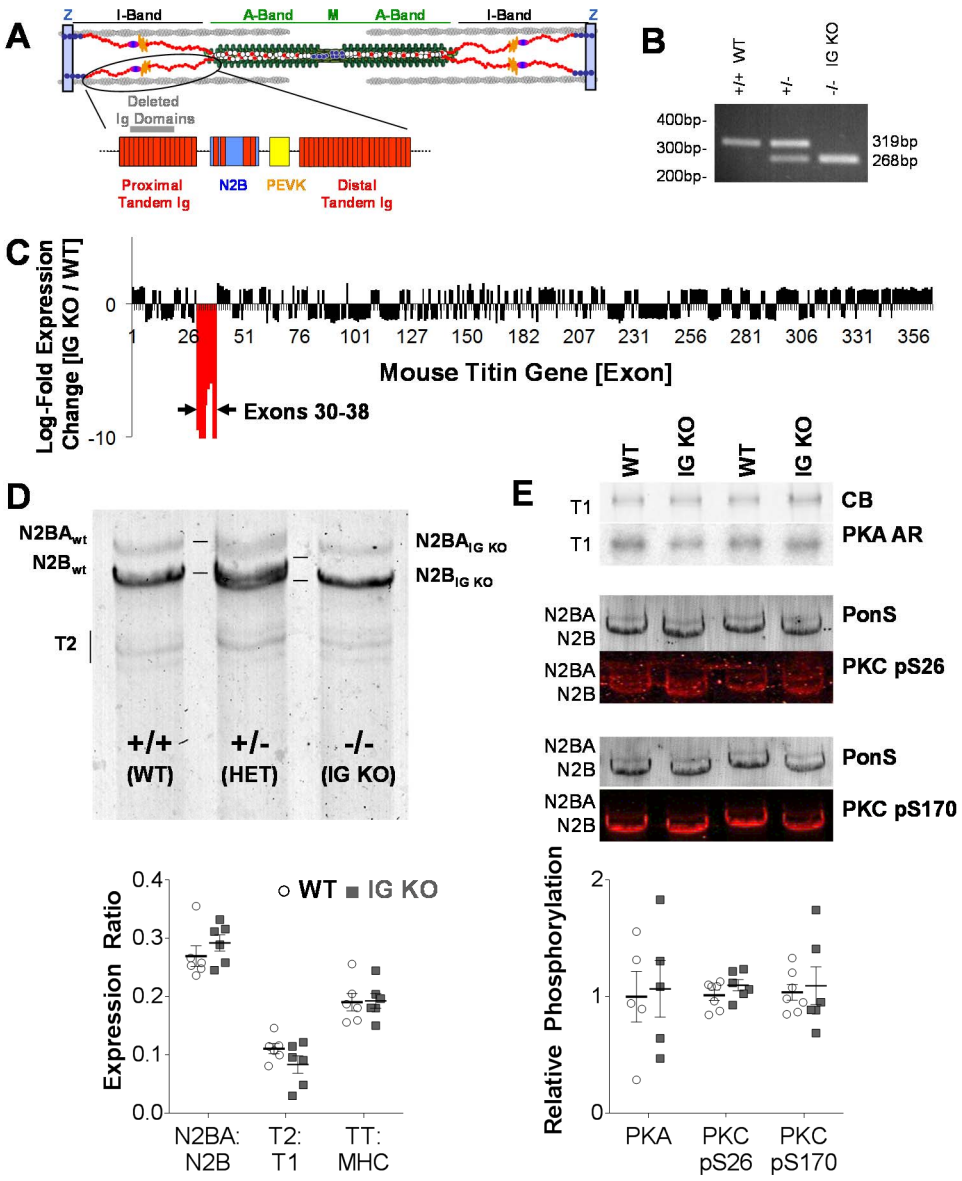

Figure S7. Basic characterization of the IG KO mouse model (Same as Fig.1 with Box-and-whiskers plots). A) Location of Ig 3-11 (deleted in the IG KO) in the spring region of titin (Ig domains are indicated by the rectangular red structures). B) PCR products showing differential gene expression from WT, heterozygous and homozygous IG KO mice. C) Titin exon microarray analysis shows titin exon expression changes only in the 9 deleted exons. D) Titin protein analysis (1% agarose gel). Top: the shortened titin (IG KO) has a higher mobility when compared to the WT titin bands and a doublet can be seen in the HET mice. Bottom: Quantitative analysis shows that titin isoform expression is unchanged (n=6). E) Titin phosphorylation is unchanged in the IG KO. Top: PKA back-phosphorylation and phospho-specific pS26 and pS170 antibodies to PKC Western blotting examples. Bottom: quantification showing unchanged phosphorylation levels in the IG KO (n=4). CB: coomassie blue; AR: autoradiography; PonS: Ponceau S. Horizontal lines denote mean±SEM.

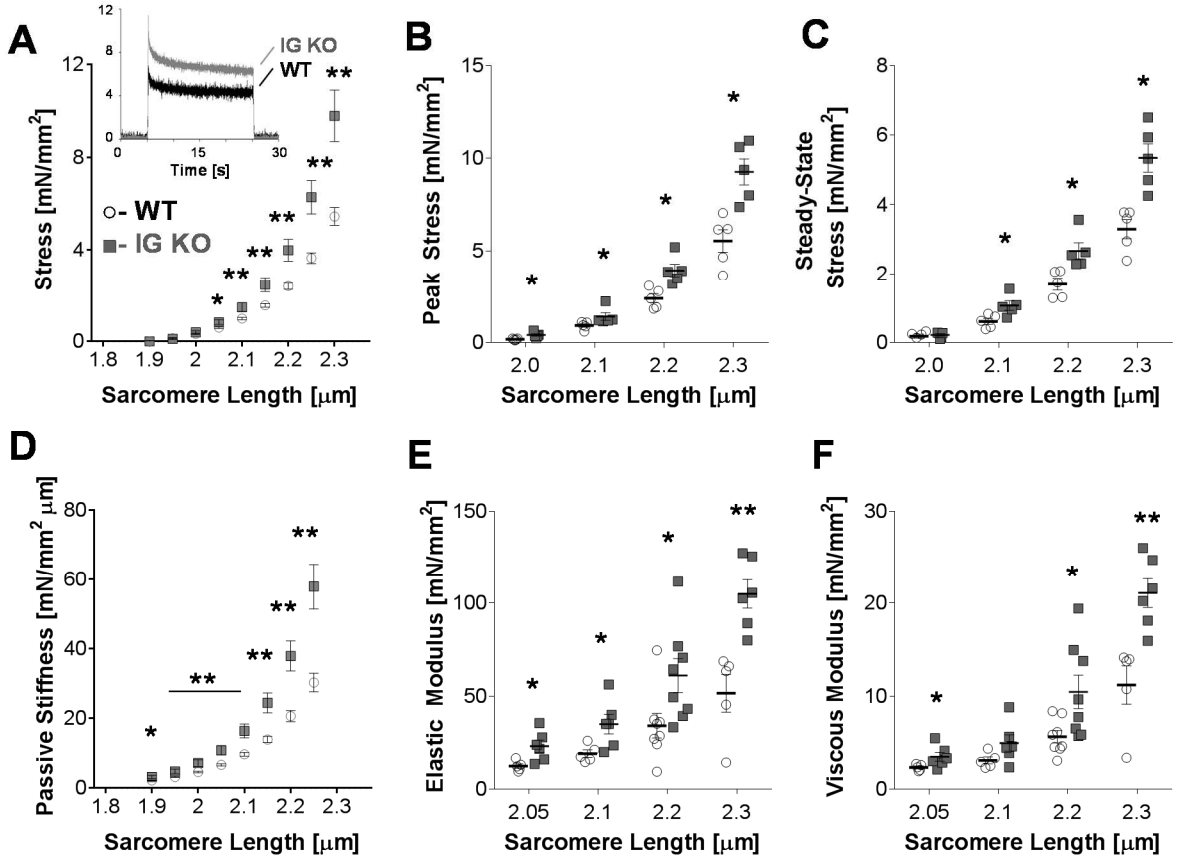

Figure S8. Cardiomyocyte mechanical properties in relaxing solution (Same as Figure 2 with Box-and-whiskers plots). A) Passive tension is higher in the IG KO cell (n=5 for WT and IG KO). Inset: Representative stretch-hold-release experiment. From these experiments, both peak stress (B) and steady state stress (C) is increased in the IG KO cells. D) Passive stiffness measured during the ramp stretch is also increased in the IG KO mouse at SLs>2.0 μm. Dynamic stiffness analysis using small amplitude sinusoidal length oscillations to determine elastic (E) and viscous (F) moduli of the myocytes. Elastic stiffness is increased at all SLs>2.0μm but viscous properties are increased only at SLs≥2.2 μm (n=6). Horizontal lines denote mean±SEM, * p<0.05; **p<0.01; ***p<0.001.

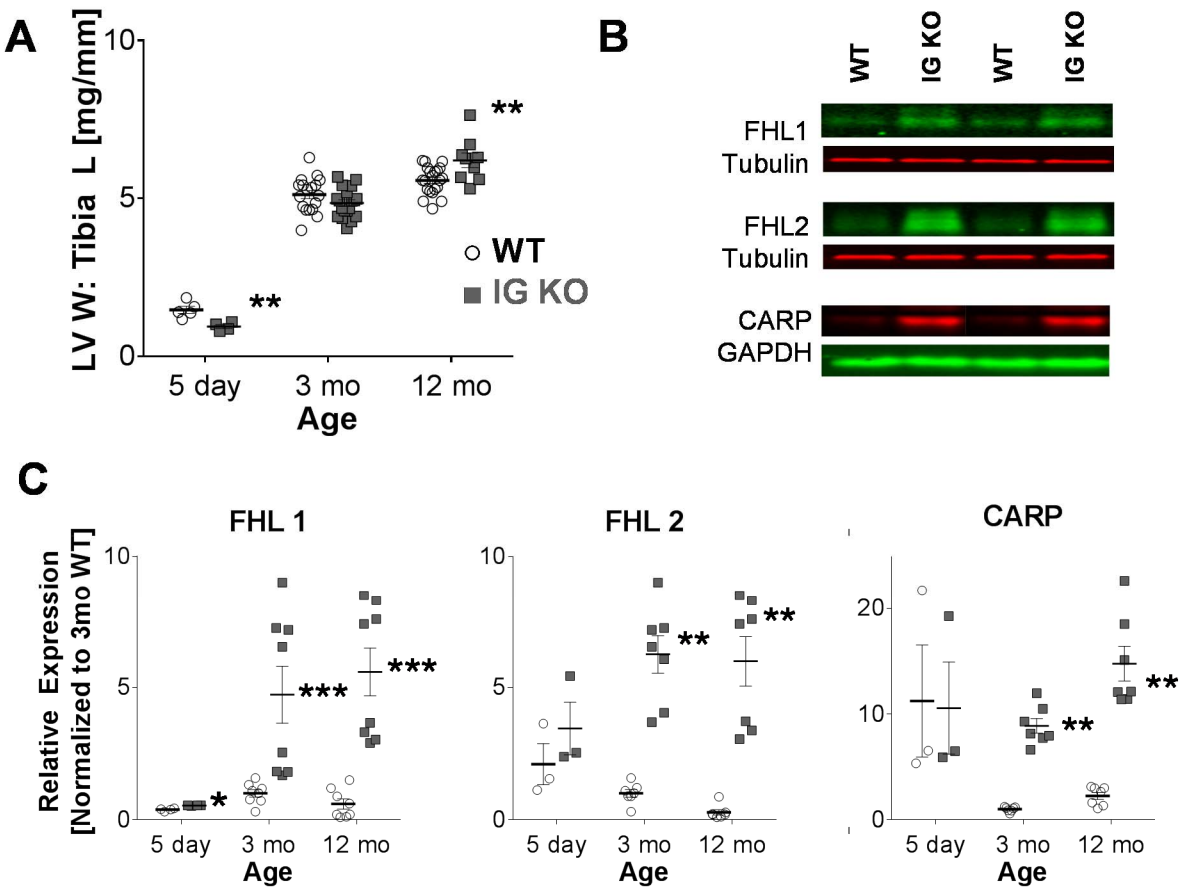

Figure S9. Cardiac Trophicity (Same as Figure 6 with Box-and-whisker plots). LVW:Tibia Length (TL) ratio is increased in older mice (A, n=6 for 5d day, n=28 for 3 mo; n=8 for 12 mo). Representative Western blots from 3mo mice (B). Expression of titin binding proteins FHL1, FHL2, and CARP were normalized to the 3mo WT (C). (n=4 for 5 day, n=8 for 3, 12 mo) Box denotes 25th and 75th percentile and whiskers display min and max, * p<0.05; ** p<0.01; ***p<0.001.

REFERENCES

1. LeWinter MM, Granzier H. Cardiac titin: A multifunctional giant. *Circulation*. 2010;121:2137-2145
2. Borlaug BA, Olson TP, Lam CSP, Flood KS, Lerman A, Johnson BD, Redfield MM. Global cardiovascular reserve dysfunction in heart failure with preserved ejection fraction. *J Am Coll Cardiol.* 2010;56:845-854
3. Lundby A, Secher A, Lage K, Nordsborg NB, Dmytriyev A, Lundby C, Olsen JV. Quantitative maps of protein phosphorylation sites across 14 different rat organs and tissues. *Nat Commun*. 2012;3:876
4. Bullard B, Ferguson C, Minajeva A, Leake MC, Gautel M, Labeit D, Ding L, Labeit S, Horwitz J, Leonard KR, Linke WA. Association of the chaperone alphab-crystallin with titin in heart muscle. *J Biol Chem*. 2004;279:7917-7924
5. Li H, Linke WA, Oberhauser AF, Carrion-Vazquez M, Kerkvliet JG, Lu H, Marszalek PE, Fernandez JM. Reverse engineering of the giant muscle protein titin. *Nature*. 2002;418:998-1002
6. Watanabe K, Muhle-Goll C, Kellermayer MS, Labeit S, Granzier H. Different molecular mechanics displayed by titin's constitutively and differentially expressed tandem ig segments. *J Struct Biol*. 2002;137:248-258
7. Zhu Y, Bogomolovas J, Labeit S, Granzier H. Single molecule force spectroscopy of the cardiac titin n2b element: Effects of the molecular chaperone alphab-crystallin with disease-causing mutations. *J Biol Chem*. 2009;284:13914-13923
8. Liu P, Jenkins NA, Copeland NG. A highly efficient recombineering-based method for generating conditional knockout mutations. *Genome Res*. 2003;13:476-484
9. Lahmers S, Wu Y, Call DR, Labeit S, Granzier H. Developmental control of titin isoform expression and passive stiffness in fetal and neonatal myocardium. *Circ Res*. 2004;94:505-513
10. Rainer J, Sanchez-Cabo F, Stocker G, Sturn A, Trajanoski Z. Carmaweb: Comprehensive r- and bioconductor-based web service for microarray data analysis. *Nucleic Acids Res.* 2006;34:W498-503
11. Hidalgo C, Hudson B, Bogomolovas J, Zhu Y, Anderson B, Greaser M, Labeit S, Granzier H. Pkc phosphorylation of titin's pevk element: A novel and conserved pathway for modulating myocardial stiffness. *Circ Res*. 2009;105:631-638
12. Warren CM, Krzesinski PR, Greaser ML. Vertical agarose gel electrophoresis and electroblotting of high-molecular-weight proteins. *Electrophoresis*. 2003;24:1695-1702
13. Hudson BD, Hidalgo CG, Gotthardt M, Granzier HL. Excision of titin's cardiac pevk spring element abolishes pkcalpha-induced increases in myocardial stiffness. *J Mol Cell Cardiol*. 2010;48:972-978
14. Yamasaki R, Wu Y, McNabb M, Greaser M, Labeit S, Granzier H. Protein kinase a phosphorylates titin's cardiac-specific n2b domain and reduces passive tension in rat cardiac myocytes. *Circulation Research.* 2002;90:1181-1188
15. Reiser PJ, Kline WO. Electrophoretic separation and quantitation of cardiac myosin heavy chain isoforms in eight mammalian species. *Am J Physiol*. 1998;274:H1048-1053
16. Chung CS, Granzier HL. Contribution of titin and extracellular matrix to passive pressure and measurement of sarcomere length in the mouse left ventricle. *J Mol Cell Cardiol*. 2011;50:731-739

17. Granzier HL, Radke MH, Peng J, Westermann D, Nelson OL, Rost K, King NMP, Yu Q, Tschöpe C, McNabb M, Larson DF, Labeit S, Gotthardt M. Truncation of titin's elastic pevk region leads to cardiomyopathy with diastolic dysfunction. *Circ Res*. 2009;105:557-564
18. Radke MH, Peng J, Wu Y, McNabb M, Nelson OL, Granzier H, Gotthardt M. Targeted deletion of titin n2b region leads to diastolic dysfunction and cardiac atrophy. *Proc Natl Acad Sci U S A*. 2007;104:3444-3449
19. Vandesompele J, De Preter K, Pattyn F, Poppe B, Van Roy N, De Paepe A, Speleman F. Accurate normalization of real-time quantitative rt-pcr data by geometric averaging of multiple internal control genes. *Genome Biol*. 2002;3:RESEARCH0034
20. Everaert BR, Boulet GA, Timmermans JP, Vrints CJ. Importance of suitable reference gene selection for quantitative real-time pcr: Special reference to mouse myocardial infarction studies. *PLoS One*. 2011;6:e23793
21. Murphy KT, Koopman R, Naim T, Leger B, Trieu J, Ibebunjo C, Lynch GS. Antibody-directed myostatin inhibition in 21-mo-old mice reveals novel roles for myostatin signaling in skeletal muscle structure and function. *FASEB J*. 2010;24:4433-4442
22. Hojayev B, Rothermel BA, Gillette TG, Hill JA. Fhl2 binds calcineurin and represses pathological cardiac growth. *Mol Cell Biol*. 2012;32:4025-4034
23. Weinert S, Bergmann N, Luo X, Erdmann B, Gotthardt M. M line-deficient titin causes cardiac lethality through impaired maturation of the sarcomere. *J Cell Biol*. 2006;173:559-570
24. Cui W, Taub DD, Gardner K. Qprimerdepot: A primer database for quantitative real time pcr. *Nucleic Acids Res*. 2007;35:D805-809
25. Toischer K, Rokita AG, Unsold B, Zhu W, Kararigas G, Sossalla S, Reuter SP, Becker A, Teucher N, Seidler T, Grebe C, Preuss L, Gupta SN, Schmidt K, Lehnart SE, Kruger M, Linke WA, Backs J, Regitz-Zagrosek V, Schafer K, Field LJ, Maier LS, Hasenfuss G. Differential cardiac remodeling in preload versus afterload. *Circulation*. 2010;122:993-1003
26. Trombitas K, Redkar A, Centner T, Wu Y, Labeit S, Granzier H. Extensibility of isoforms of cardiac titin: Variation in contour length of molecular subsegments provides a basis for cellular passive stiffness diversity. *Biophys J*. 2000;79:3226-3234
27. Stewart JA, Jr., Wei CC, Brower GL, Rynders PE, Hankes GH, Dillon AR, Lucchesi PA, Janicki JS, Dell'Italia LJ. Cardiac mast cell- and chymase-mediated matrix metalloproteinase activity and left ventricular remodeling in mitral regurgitation in the dog. *J Mol Cell Cardiol*. 2003;35:311-319
28. King NMP, Methawasin M, Nedrud J, Harrell N, Chung CS, Helmes M, Granzier H. Mouse intact cardiac myocyte mechanics: Cross-bridge and titin-based stress in unactivated cells. *J Gen Physiol*. 2011;137:81-91
29. Chung CS, Methawasin M, Nelson OL, Radke MH, Hidalgo CG, Gotthardt M, Granzier HL. Titin based viscosity in ventricular physiology: An integrative investigation of pevk-actin interactions. *J Mol Cell Cardiol*. 2011;51:428-434
30. Wu Y, Cazorla O, Labeit D, Labeit S, Granzier H. Changes in titin and collagen underlie diastolic stiffness diversity of cardiac muscle. *J Mol Cell Cardiol*. 2000;32:2151-2162
31. Granzier HL, Irving TC. Passive tension in cardiac muscle: Contribution of collagen, titin, microtubules, and intermediate filaments. *Biophys J*. 1995;68:1027-1044

32. Granzier HL, Wang K. Interplay between passive tension and strong and weak binding cross-bridges in insect indirect flight muscle. A functional dissection by gelsolin-mediated thin filament removal. *J Gen Physiol*. 1993;101:235-270
33. Weber KT, Janicki JS, Reeves RC, Hefner LL. Factors influencing left ventricular shortening in isolated canine heart. 1976;230:419-426
34. Konhilas JP, Maass AH, Luckey SW, Stauffer BL, Olson EN, Leinwand LA. Sex modifies exercise and cardiac adaptation in mice. *Am J Physiol Heart Circ Physiol.* 2004;287:H2768-2776
35. Burkhoff D, Mirsky I, Suga H. Assessment of systolic and diastolic ventricular properties via pressure-volume analysis: A guide for clinical, translational, and basic researchers. *Am J Physiol Heart Circ Physiol.* 2005;289:H501-512
36. Kellermayer MS, Smith SB, Bustamante C, Granzier HL. Complete unfolding of the titin molecule under external force. *J Struct Biol*. 1998;122:197-205
37. Watanabe K, Nair P, Labeit D, Kellermayer MS, Greaser M, Labeit S, Granzier H. Molecular mechanics of cardiac titin's pevk and n2b spring elements. *J Biol Chem.* 2002;277:11549-11558.
38. Trombitas K, Freiburg A, Centner T, Labeit S, Granzier H. Molecular dissection of n2b cardiac titin's extensibility. *Biophys J*. 1999;77:3189-3196